NANO LETTERS

pubs.acs.org/NanoLett

Letter

Enhanced Thermoelectricity in Metal−[60]Fullerene−Graphene Molecular Junctions

Simon A. Svatek,[#] Valentina Sacchetti,[#] Laura Rodríguez-Pérez, Beatriz M. Illescas, Laura Rincón-García, Gabino Rubio-Bollinger, M. Teresa González, Steven Bailey, Colin J. Lambert,* Nazario Martín,* and Nicolás Agraït*

Cite This: *Nano Lett.* 2023, 23, 2726−2732

Read Online

ACCESS | Metrics & More | Article Recommendations | Supporting Information

ABSTRACT: The thermoelectric properties of molecular junctions consisting of a metal Pt electrode contacting [60]fullerene derivatives covalently bound to a graphene electrode have been studied by using a conducting-probe atomic force microscope (c-AFM). The [60]fullerene derivatives are covalently linked to the graphene via two *meta*-connected phenyl rings, two *para*-connected phenyl rings, or a single phenyl ring. We find that the magnitude of the Seebeck coefficient is up to nine times larger than that of Au−C_{60}−Pt molecular junctions. Moreover, the sign of the thermopower can be either positive or negative depending on the details of the binding geometry and on the local value of the Fermi energy. Our results demonstrate the potential of using graphene electrodes for controlling and enhancing the thermoelectric properties of molecular junctions and confirm the outstanding performance of [60]fullerene derivatives.

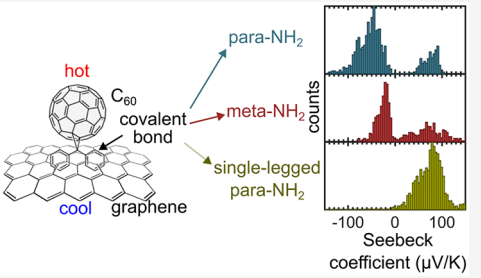

KEYWORDS: *thermoelectricity, quantum thermopower, fullerenes, molecular electronics, conductive atomic force microscopy*

Graphene and [60]fullerene are two Nobel laureated disruptive materials representing new allotropes of carbon whose properties could be fine-tuned upon chemical covalent[1,2] or supramolecular modification.[3,4] Therefore, the construction of novel fullerene−graphene architectures could enhance the existing properties of both carbon allotropes and/or bring about new and exciting ones.[5] In this regard, several [60]fullerene-graphene hybrids have been reported in the references.[6−10] It is worth noting that, as expected, the covalent wet modification of graphene involves the functionalization on both sides of the graphene layer. However, functionalization of only one side has also been accomplished by using a solid substrate where the graphene layer is deposited.[11−13] In this sense, in most of the practical applications of graphene, it is actually supported on a solid substrate which could be easily incorporated into an electronic device. Therefore, the chemical functionalization of graphene on a substrate with [60]fullerene may drastically expand the material capabilities by fine-tuning its chemical and physical properties.

Studies of the thermoelectric properties of molecular junctions consisting of organic molecules connected to electrodes provide insight into the charge transport mechanisms at the molecular level.[14] They also open the possibility of designing new thermoelectric devices with enhanced thermoelectric properties that could find applications in energy management, on-chip cooling, temperature sensing, or energy harvesting.[15−20] All-carbon hybrid devices show great promise in their ability to exploit desirable thermoelectric properties.[21−25] One such property is the delicate control of the sign and magnitude of the Seebeck coefficient. This control has been demonstrated, for example, by applying tip pressure to modulate the coupling of the molecule to the electrode[26] and by tuning intermolecular interactions between C_{60} molecules.[18]

The thermopower of various single fullerene molecules between a gold substrate and a metal tip of Au, Ag, and Pt was studied by Yee et al.[27] They found that for C_{60}, PCBM, and C_{70}, the Seebeck coefficient was negative, being largest in magnitude for C_{70} and for the Ag tip (−33 μV/K). These are among the highest measured values for molecular junctions.[14] Evangeli et al.[18] found that the thermopower of C_{60} dimers between gold electrodes reaches values of −33 μV/K, almost double that of C_{60} (−18 μV/K). The fact that the thermopower is negative for all these fullerene molecular junctions shows that electron transport takes place through their LUMOs (lowest unoccupied molecular orbitals). In contrast, it has been shown that, in molecular junctions of endohedral fullerenes, the Seebeck coefficient can be either

Received: January 2, 2023
Revised: March 14, 2023
Published: March 27, 2023

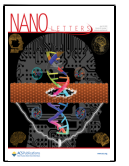

https://doi.org/10.1021/acs.nanolett.3c00014
Nano Lett. 2023, 23, 2726−2732

positive or negative depending on the orientation of the encapsulated moiety and also in response to pressure; this behavior was explained by the presence of transmission resonances close to the Fermi level.[17]

Here, we investigate the thermoelectric properties of single-molecule junctions formed by contacting diphenylmethano-fullerene molecules (**1**−**3**) bound covalently to graphene on SiO_2/Si (**GOS-1**, **GOS-2**, and **GOS-3**) as shown in Figure 1a.

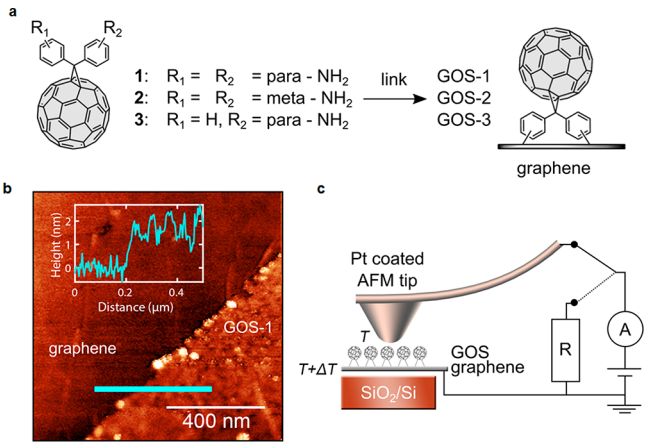

Figure 1. (a) Scheme of the three molecules studied (**1**−**3**) and their covalent link to graphene. (b) AFM topographic image of the edge of an island of **GOS-1** and one profile showing its apparent height. (c) Scheme of the setup for the measurement of the thermoelectric properties.

We find that the Seebeck coefficients of these molecular junctions present typical values of up to 74 μV/K and −56 μV/K, which are much larger in magnitude than the 8.9 μV/K previously reported for single Au−C_{60}−Pt junctions. We use density functional theory (DFT) calculations to obtain a detailed understanding of the origin of these values and the molecular configurations responsible for these amazing behaviors.

RESULTS AND DISCUSSION

For the study of the thermoelectric properties, we employed large area monolayer graphene grown by chemical vapor deposition (CVD) on copper foils, cut into smaller pieces and transferred onto SiO_2. Covalent binding of methanofullerenes **1**−**3** to graphene on substrate (GOS) led to derivatives **GOS-1**, **GOS-2**, and **GOS-3** (Scheme 1). The synthesis of compounds **1**−**3** was carried out employing a Bamford−Stevens reaction, which takes place through the *in situ* generation of intermediate diazocompounds with sodium methoxide in the presence of pyridine and [60]fullerene in refluxing *o*-dichlorobenzene (*o*-DCB), affording the final amino or diamino-containing diphenylmethanofullerenes **1**−**3**.[28] The covalent functionalization of GOS was conducted via aryl diazonium chemistry in the presence of isoamyl nitrite, following a slightly modified protocol of that previously reported by Tour and co-workers.[29] Thus, the corresponding aryl diazonium salts are generated in advance by adding isoamyl nitrite to a solution of **1**, **2**, or **3** and subsequently drop casted on the GOS. As proof of concept and to validate the covalent functionalization over the graphene grafted on top of SiO_2/Si, we have also synthesized the analogous all-carbon hybrid materials over few layers graphene (FLG) to achieve a complete characterization of the final derivatives. Pristine FLG was obtained through graphite exfoliation following Colleman's method with a high degree of purity.[30] A suspension of FLG in *o*-DCB was immediately reacted with [60]fullerene derivatives **1** and **2** in the presence of isoamyl nitrite providing **FLG-1** and **FLG-2,** respectively (Scheme 1).

Raman spectroscopy under 532 nm laser wavelengths gives insights of the surface functionalization of FLG and GOS. All aggregates present an increase in the D-band with respect to the G-band, which is generally associated with a higher defect

Scheme 1. Covalent Functionalization of FLG and GOS through Tour's Reaction

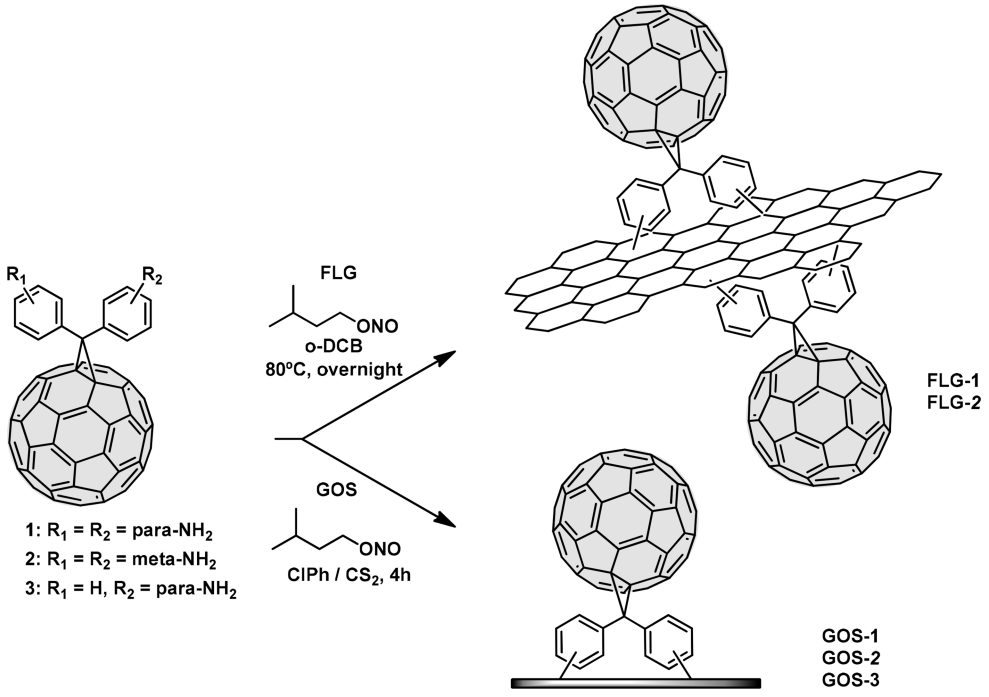

https://doi.org/10.1021/acs.nanolett.3c00014
Nano Lett. 2023, 23, 2726−2732

degree on the nanomaterials, also attributed to functionalization. This increase is related with a substantial rehybridization from sp^2 carbon atoms to sp^3 as a result of the covalent attachment of **1**, **2**, or **3**, respectively. Therefore, the ratio with the G band I_D/I_G is a way to quantify the covalent functionalization degree of those materials. According to this criterion, in our measurement we found I_D/I_G ratios of 0.26 for **GOS-1**, 0.54 for **GOS-2**, and 0.23 for **GOS-3** (Figure 2 and Figures S1−S3). Moreover, a new peak around 1457 cm^{-1} is clearly observed for all fullerene aggregates which can be assigned to the pentagonal pinch mode [Ag(2)] of C_{60}.[31] These results indicate a higher functionalization in the case of **GOS-2**, which is also confirmed by the observed I_D/I_G ratios for **FLG-1** and **FLG-2** (Figure S4). Thus, this evidence confirms the covalent attachment of **1**, **2**, or **3** on the FLG or GOS. A characterization of **FLG-1** and **FLG-2** employing ATG, FTIR, XPS, and TEM has been carried out and is available in the SI.

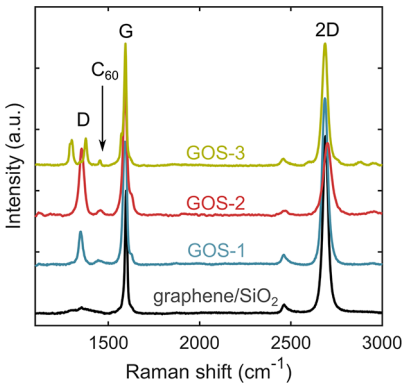

Figure 2. Raman spectra of pristine GOS (black), GOS-1 (blue), GOS-2 (red), and GOS-3 (green) under 532 nm laser excitation wavelength.

AFM images of the samples reveal the formation of micrometer-sized molecular islands of **GOS-1**, **GOS-2**, or **GOS-3** that partially cover the graphene sheet (see Figure 1b). The measured height is around 2 nm, which is larger than the diameter of a [60]fullerene and consistent with the covalent bonding between the fullerene and graphene.

To characterize the thermoelectric response of the [60]-fullerene derivatives on graphene, we used a conductive atomic force microscope (c-AFM) with Pt-coated tips (Multi75-G from BudgetSensors). Figure 1c shows a scheme of the measuring technique, which we have previously described in detail.[18] In short, the substrate is heated and the tip−substrate temperature difference ΔT is determined from direct measurements of the temperatures of the cantilever chip and the substrate. The Pt-coated tip is placed into gentle contact (∼30 nN) with the substrate and held stationary through a feedback loop controller. This allows us to measure current−voltage (I−V) characteristics in which the thermoelectric voltage shows as a voltage-offset ΔV, from which one can obtain the thermopower or Seebeck coefficient $S = -\Delta V/\Delta T$. A zero-calibration of the voltage reading is performed in short time intervals by disconnecting the c-AFM from the V source and connecting a resistor R instead, facilitating a precise voltage reading. Then we can determine S and the conductance G (from the slope of the I−V curves) for a number of given points on the substrate.

Figure 3a shows a histogram of S measured with the tip in contact with the graphene. We obtain a very small average value of 2 μV/K, corresponding to the thermopower of the Pt-tip/graphene/SiO_2 junction. This measurement configuration is totally different to that of previously reported experiments that determine the in-plane thermopower of graphene, which is found to be between −50 and +50 μV/K, depending on doping.[32]

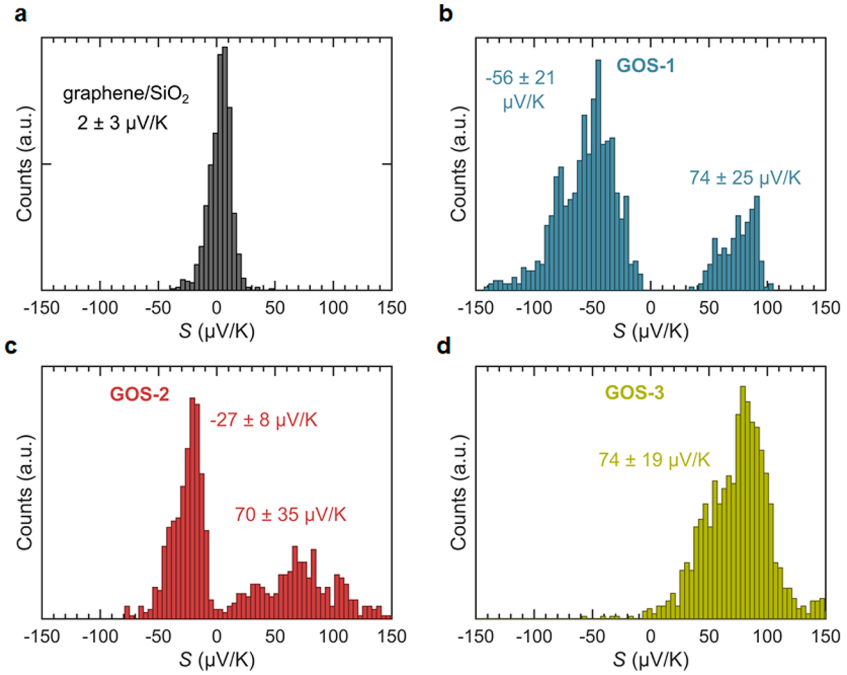

Figure 3. Histograms of the thermopower of junctions formed with (a) graphene, (b) **GOS-1**, (c) **GOS-2**, and (d) **GOS-3**. The uncertainty given for the Seebeck coefficients equals the standard deviation of the distribution of measured values.

https://doi.org/10.1021/acs.nanolett.3c00014
Nano Lett. 2023, 23, 2726−2732

Measurements of the thermopower of **GOS-1** yield two distinct sets of values centered on $S = -56\ \mu V/K$ and $S = 74\ \mu V/K$ (see Figure 3b). Note that, for a single approach in a given area, only values that correspond to one of the peaks appear, although imaging shows no significant difference between areas of different thermopowers. These Seebeck values are exceptionally high compared with those commonly observed in molecular junctions of other organic molecules.[14] Interestingly, we find that when the force with which the tip is pushed toward the surface is increased, the tip displaces the molecules, jumps into contact with the graphene, and registers the Seebeck coefficient of graphene, as shown in Figure 3a. Similarly for **GOS-2**, we observe two peaks in the thermopower histogram, centered on $S = -27\ \mu V/K$ and $S = 70\ \mu V/K$ (see Figure 3c).

The presence of broad distributions with two peak values of the Seebeck coefficient for both **GOS-1** and **GOS-2** suggests the existence of different configurations, in particular the possibility of having molecules bound by the two legs or only by one leg. To test this hypothesis, we prepared samples of **GOS-3**, which can bind with only one leg. Figure 3d shows a histogram of the Seebeck coefficient S measured when the tip is in contact with an island of **GOS-3** on graphene. We only find high positive values of S centered around $S = 74\ \mu V/K$.

To further understand this behavior, we used density functional theory (DFT) combined with quantum transport theory to compute the electrical conductance G and Seebeck coefficient S of these junctions. Initially, the SIESTA implementation of DFT was used to extract the mean field Hamiltonian of the system for the relaxed geometries shown in Figure 4. The electronic and thermoelectric properties were then calculated using the transport code GOLLUM, starting from the transmission coefficients $T(E)$, as described in the SI.

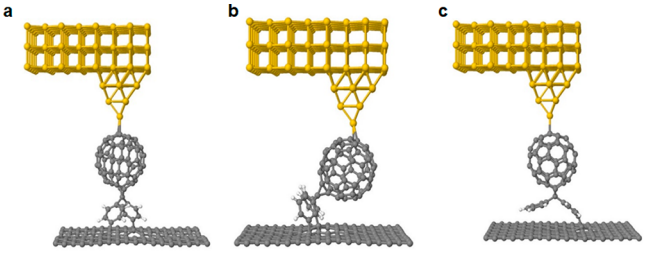

Figure 4. DFT-generated structures of (a) **GOS-1**, (b) **GOS-2**, and (c) **GOS-3** covalently bonded to a graphene sheet. As an archetypal metallic electrode, the top contact (shown in yellow) is chosen to be gold and is attached via a tapered tip to a stable contact point on the C_{60}. The processes involved in creating these structures are described in detail in the SI.

As discussed in the SI, the calculated Seebeck coefficients were found to be sensitive to the location of the metallic tip on the surface of the C_{60} and to the value of the Fermi energy, which can vary across the film due to the presence of adsorbates, such as water. Therefore, values of S for a range of tip-C_{60} contact locations and a range of Fermi energies were calculated. These were then used to create the histograms of Seebeck coefficients shown in Figure 5. These are in qualitative agreement with the experimental histograms of Figure 3, with **GOS-3** values of S being positive, whereas **GOS-1** and **GOS-2** histograms possess peaks at both positive and negative values. This suggests that the existence of two peaks in the histograms cannot be considered as an indication of the presence of molecules bound by one or two legs and that the precise shape of Seebeck histograms depends on the range of Fermi energies and tip-C_{60} configurations sampled in the experiments. The sign of the Seebeck coefficient depends on the energetic location of the frontier orbitals relative to the Fermi energy. If the LUMO is closer to the Fermi energy, then the Seebeck coefficient is negative, whereas if the HOMO is closer, the Seebeck coefficient is positive. Bonding of the tip to the unattached phenyl ring was not considered, since the unattached ring points toward the substrate, making it unavailable to the tip.

In the above simulations, each junction contained a single molecule, whereas in the experiments, many molecules are present. The effect of intermolecular interactions in junctions with more than one C_{60} has been considered in a previous work.[33] This study showed that intermolecular interactions cause small changes in the Seebeck coefficient, but these are negligible compared to the sample-to-sample fluctuations shown in Figures 3 and 5.

In summary, suitably functionalized [60]fullerene derivatives (**1**−**3**) have been covalently linked to 2D graphene either through two *meta*-connected phenyl rings, two *para*-connected phenyl rings, or just a single phenyl ring, resulting in the new systems **GOS1**−**3**. All the [60]fullerene/graphene hybrids have been characterized by spectroscopic and microscopic techniques, revealing the efficient covalent linkage between the two carbon allotropes.

Our work demonstrates that the [60]fullerene derivatives **GOS-1**, **GOS-2**, and **GOS-3** generate exceptionally high quantum thermopowers when covalently anchored to graphene, thus suggesting great promise for molecular/graphene composite materials in thermoelectric applications. The possibility to change the sign of the most probable Seebeck coefficient when utilizing two anchoring groups implies potential for tailoring thermoelectric performance in more complex device architectures in which positive and negative contributions may be combined to build thermoelectric modules.

DFT calculations show that the sign of the Seebeck coefficient of **GOS-1** and **GOS-2** is very sensitive to local variations of the Fermi level, leading to both positive and negative values of the Seebeck coefficient. In contrast, the calculations predict that, for the same local variations in the Fermi energy, the thermopower of **GOS-3** is more robust when anchored to graphene, since its transmission function exhibits a consistently negative slope around the energy range of interest. Fluctuations in energies of the frontier orbitals relative to the Fermi energy are modeled by sampling a range of Fermi energies. The precise range sampled experimentally is unknown, because small changes in the bonding configuration and defects in the graphene will change the Fermi energy relative to frontier orbital energies. Therefore, we sampled a range, which was consistent with experiment. In this sense, although the theory is not predictive, we are able to show that the experiment can be consistent with theory. In conclusion, the geometries and Fermi energies vary so much that a broad distribution of Seebeck coefficients are observed. The sign of the Seebeck coefficient depends on the energetic location of the frontier orbitals relative to the Fermi energy. These are shifted relative to their gas-phase values by the real part of the self-energy, due to contact with the substrate and tip. This shift depends on the strength of the contact, which in turn depends on the orientation of the molecule and details of the linker.

https://doi.org/10.1021/acs.nanolett.3c00014
Nano Lett. 2023, 23, 2726−2732

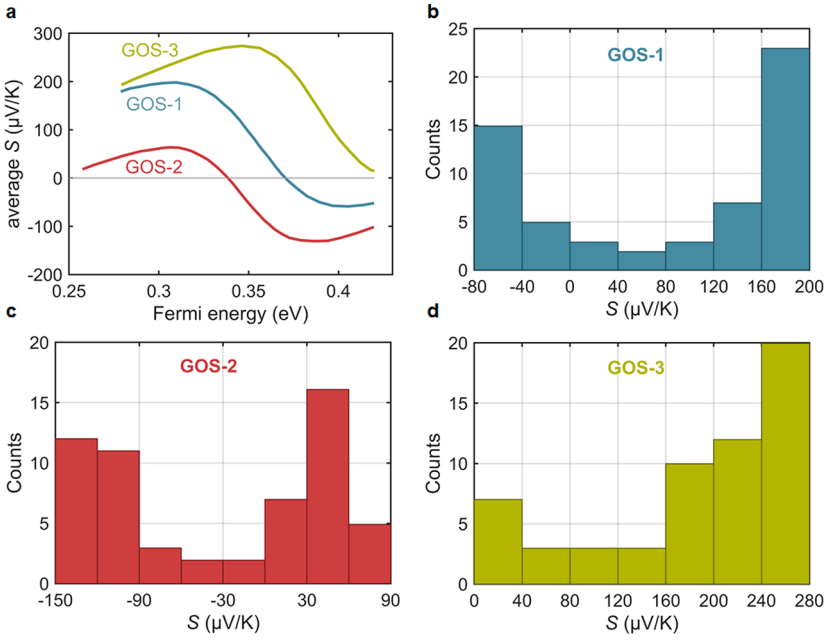

Figure 5. (a) Dependence of the average S versus Fermi energy for 20 different tip−C_{60} contact geometries for **GOS-1**, **GOS-2**, and **GOS-3** (in black, red, and green, respectively). (b−d) Histograms of the Seebeck coefficient for these 20 different contact geometries for **GOS-1**, **GOS-2**, and **GOS-3**, respectively. The histograms are obtained by sampling the Seebeck coefficient at different Fermi energies between 0.35 and 0.42 eV, relative to the DFT-predicted Fermi energy E_F^{DFT} (as shown in Figure S18).

Random energy level shifts also occur due to imperfections in the graphene substrate.

■ ASSOCIATED CONTENT

Supporting Information

The Supporting Information is available free of charge at https://pubs.acs.org/doi/10.1021/acs.nanolett.3c00014.

Details about synthesis and further characterization, spectroscopic data, thermogravimetric analysis, transmission electron microscopy, and computational details (PDF)

■ AUTHOR INFORMATION

Corresponding Authors

Colin J. Lambert − *Department of Physics, Lancaster University, Lancaster LA1 4YW, United Kingdom;* orcid.org/0000-0003-2332-9610; Email: c.lambert@lancaster.ac.uk

Nazario Martín − *Instituto Madrileño de Estudios Avanzados en Nanociencia (IMDEA-Nanociencia), 28049 Madrid, Spain; Organic Chemistry Department, Faculty of Chemistry, Universidad Complutense de Madrid, E-28040 Madrid, Spain;* Email: nazmar@ucm.es

Nicolás Agraït − *Instituto Madrileño de Estudios Avanzados en Nanociencia (IMDEA-Nanociencia), 28049 Madrid, Spain; Departamento de Física de la Materia Condensada, Facultad de Ciencias, Universidad Autónoma de Madrid, 28049 Madrid, Spain; Condensed Matter Physics Center (IFIMAC) and Instituto Universitario de Ciencia de Materiales "Nicolás Cabrera" (INC), Facultad de Ciencias, Universidad Autónoma de Madrid, 28049 Madrid, Spain;* orcid.org/0000-0003-4840-5851; Email: nicolas.agrait@uam.es

Authors

Simon A. Svatek − *Instituto Madrileño de Estudios Avanzados en Nanociencia (IMDEA-Nanociencia), 28049 Madrid, Spain; Departamento de Física de la Materia Condensada, Facultad de Ciencias, Universidad Autónoma de Madrid, 28049 Madrid, Spain;* Present Address: (S.A.S.) Instituto de Energía Solar, Universidad Politécnica de Madrid, Avenida Complutense 30, 28040 Madrid, Spain; orcid.org/0000-0002-8104-1888

Valentina Sacchetti − *Instituto Madrileño de Estudios Avanzados en Nanociencia (IMDEA-Nanociencia), 28049 Madrid, Spain; Organic Chemistry Department, Faculty of Chemistry, Universidad Complutense de Madrid, E-28040 Madrid, Spain*

Laura Rodríguez-Pérez − *Organic Chemistry Department, Faculty of Chemistry, Universidad Complutense de Madrid, E-28040 Madrid, Spain*

Beatriz M. Illescas − *Organic Chemistry Department, Faculty of Chemistry, Universidad Complutense de Madrid, E-28040 Madrid, Spain;* orcid.org/0000-0002-4727-8291

Laura Rincón-García − *Departamento de Física de la Materia Condensada, Facultad de Ciencias, Universidad Autónoma de Madrid, 28049 Madrid, Spain;* orcid.org/0000-0002-2408-0928

Gabino Rubio-Bollinger − *Departamento de Física de la Materia Condensada, Facultad de Ciencias, Universidad Autónoma de Madrid, 28049 Madrid, Spain; Condensed Matter Physics Center (IFIMAC) and Instituto Universitario de Ciencia de Materiales "Nicolás Cabrera" (INC), Facultad de Ciencias, Universidad Autónoma de Madrid, 28049 Madrid, Spain;* orcid.org/0000-0001-7864-8980

M. Teresa González − *Instituto Madrileño de Estudios Avanzados en Nanociencia (IMDEA-Nanociencia), 28049 Madrid, Spain;* orcid.org/0000-0002-7253-797X

Steven Bailey − *Department of Physics, Lancaster University, Lancaster LA1 4YW, United Kingdom*

https://doi.org/10.1021/acs.nanolett.3c00014
Nano Lett. 2023, 23, 2726−2732

Complete contact information is available at:
https://pubs.acs.org/10.1021/acs.nanolett.3c00014

Author Contributions

#(S.A.S. and V.S.) These authors contributed equally. V.S. and L.R.-P. synthesized the molecules and the materials and characterized the samples using TGA, Raman, IR, XPS, and TEM techniques. S.A.S., L.R.-G., G.R.B., M.T.G., and N.A. developed the cAFM setup, and S.A.S. carried out the cAFM experiments. S.B. and C.J.L. provided theory and carried out the transport and DFT modeling. The manuscript was written by B.M.I., S.A.S., N.M., C.J.L., and N.A. All authors contributed to data analysis and edited the manuscript. All authors have given approval to the final version of the manuscript.

Notes

The authors declare no competing financial interest.

■ ACKNOWLEDGMENTS

This work has been supported by the European Commission through FP7 ITN MOLESCO (Project Number 606728), the (MAD2D-CM)-UCM1-MRR project and through the EC H2020 FET Open Project Grant Agreement Number 767187 "QuIET". The authors acknowledge support from the Spanish Ministry of Science and Innovation MCIN (Projects PID2020-114653RB-I00, PID2020-115120GB-I00, Centro de Excelencia Severo Ochoa SEV-2016-0686). L.R.-G. acknowledges support from Spanish MECD (Grant No. FPU14/03368) and, with N.A., funding from the Education and Research Council of the Comunidad de Madrid and the European Social Fund (ref. PEJD-2019-POST/IND-16353).

■ REFERENCES

(1) Vacchi, I. A.; Ménard-Moyon, C.; Bianco, A. Chemical Functionalization of Graphene Family Members. *Phys. Sci. Rev.* **2017**, *2* (1), 20160103.
(2) Bottari, G.; Herranz, M. Á.; Wibmer, L.; Volland, M.; Rodríguez-Pérez, L.; Guldi, D. M.; Hirsch, A.; Martín, N.; D'Souza, F.; Torres, T. Chemical functionalization and characterization of graphene-based materials. *Chem. Soc. Rev.* **2017**, *46* (15), 4464−4500.
(3) Garrido, M.; Volland, M. K.; Münich, P. W.; Rodríguez-Pérez, L.; Calbo, J.; Ortí, E.; Herranz, M. Á.; Martín, N.; Guldi, D. M. Mono- and Tripodal Porphyrins: Investigation on the Influence of the Number of Pyrene Anchors in Carbon Nanotube and Graphene Hybrids. *J. Am. Chem. Soc.* **2020**, *142* (4), 1895−1903.
(4) Bao, L.; Zhao, B.; Ali, M.; Assebban, M.; Yang, B.; Kohring, M.; Ryndyk, D.; Heine, T.; Weber, H. B.; Halik, M.; Hauke, F.; Hirsch, A. Hierarchical Assembly and Sensing Activity of Patterned Graphene-Hamilton Receptor Nanostructures. *Adv. Mater. Interfaces* **2022**, *9* (16), 2200425.
(5) Pérez, E. M.; Martín, N. $\pi-\pi$ interactions in carbon nanostructures. *Chem. Soc. Rev.* **2015**, *44* (18), 6425−6433.
(6) Chen, M.; Guan, R.; Yang, S. Hybrids of Fullerenes and 2D Nanomaterials. *Adv. Sci.* **2019**, *6* (1), 1800941.
(7) Wei, T.; Martin, O.; Yang, S.; Hauke, F.; Hirsch, A. Modular Covalent Graphene Functionalization with C_{60} and the Endohedral Fullerene $Sc_3N@C_{80}$: A Facile Entry to Synthetic-Carbon-Allotrope Hybrids. *Angew. Chem., Int. Ed.* **2019**, *58* (3), 816−820.
(8) Garrido, M.; Calbo, J.; Rodríguez-Pérez, L.; Aragó, J.; Ortí, E.; Herranz, M. Á.; Martín, N. Non-covalent graphene nanobuds from mono- and tripodal binding motifs. *Chem. Commun.* **2017**, *53* (92), 12402−12405.
(9) Muñoz, A.; Rodríguez-Pérez, L.; Casado, S.; Illescas, B. M.; Martín, N. Multivalent fullerene/π-extended TTF electroactive molecules − non-covalent interaction with graphene and charge transfer implications. *J. Mater. Chem. C* **2019**, *7* (29), 8962−8968.
(10) García, D.; Rodríguez-Pérez, L.; Herranz, M. A.; Peña, D.; Guitián, E.; Bailey, S.; Al-Galiby, Q.; Noori, M.; Lambert, C. J.; Pérez, D.; Martín, N. A C_{60}-aryne building block: synthesis of a hybrid all-carbon nanostructure. *Chem. Commun.* **2016**, *52* (40), 6677−6680.
(11) Wetzl, C.; Silvestri, A.; Garrido, M.; Hou, H.-L.; Criado, A.; Prato, M. The Covalent Functionalization of Surface-Supported Graphene: An Update. *Angew. Chem., Int. Ed.* **2023**, *62* (6), e202212857.
(12) Al-Fogra, S.; Yang, B.; Jurkiewicz, L.; Hauke, F.; Hirsch, A.; Wei, T. Spatially Resolved Janus Patterning of Graphene by Direct Laser Writing. *J. Am. Chem. Soc.* **2022**, *144* (43), 19825−19831.
(13) Bao, L.; Kohring, M.; Weber, H. B.; Hauke, F.; Hirsch, A. Covalently Doped Graphene Superlattices: Spatially Resolved Supratopic- and Janus-Binding. *J. Am. Chem. Soc.* **2020**, *142* (37), 16016−16022.
(14) Rincón-García, L.; Evangeli, C.; Rubio-Bollinger, G.; Agraït, N. Thermopower measurements in molecular junctions. *Chem. Soc. Rev.* **2016**, *45* (15), 4285−4306.
(15) Paulsson, M.; Datta, S. Thermoelectric effect in molecular electronics. *Phys. Rev. B* **2003**, *67* (24), 241403.
(16) Aradhya, S. V.; Venkataraman, L. Single-molecule junctions beyond electronic transport. *Nat. Nanotechnol.* **2013**, *8* (6), 399−410.
(17) Rincón-García, L.; Ismael, A. K.; Evangeli, C.; Grace, I.; Rubio-Bollinger, G.; Porfyrakis, K.; Agraït, N.; Lambert, C. J. Molecular design and control of fullerene-based bi-thermoelectric materials. *Nat. Mater.* **2016**, *15* (3), 289−293.
(18) Evangeli, C.; Gillemot, K.; Leary, E.; González, M. T.; Rubio-Bollinger, G.; Lambert, C. J.; Agraït, N. Engineering the Thermopower of C_{60} Molecular Junctions. *Nano Lett.* **2013**, *13* (5), 2141−2145.
(19) Ke, S.-H.; Yang, W.; Curtarolo, S.; Baranger, H. U. Thermopower of Molecular Junctions: An ab Initio Study. *Nano Lett.* **2009**, *9* (3), 1011−1014.
(20) Lambert, C. J. Basic concepts of quantum interference and electron transport in single-molecule electronics. *Chem. Soc. Rev.* **2015**, *44* (4), 875−888.
(21) Sadeghi, H.; Sangtarash, S.; Lambert, C. J. Enhanced Thermoelectric Efficiency of Porous Silicene Nanoribbons. *Sci. Rep.* **2015**, *5* (1), 9514.
(22) Al-Galiby, Q. H.; Sadeghi, H.; Algharagholy, L. A.; Grace, I.; Lambert, C. Tuning the thermoelectric properties of metallo-porphyrins. *Nanoscale* **2016**, *8* (4), 2428−2433.
(23) Karamitaheri, H.; Pourfath, M.; Faez, R.; Kosina, H. Geometrical effects on the thermoelectric properties of ballistic graphene antidot lattices. *J. Appl. Phys.* **2011**, *110* (5), 054506.
(24) Sadeghi, H.; Sangtarash, S.; Lambert, C. J. Oligoyne Molecular Junctions for Efficient Room Temperature Thermoelectric Power Generation. *Nano Lett.* **2015**, *15* (11), 7467−7472.
(25) Karamitaheri, H.; Neophytou, N.; Pourfath, M.; Faez, R.; Kosina, H. Engineering enhanced thermoelectric properties in zigzag graphene nanoribbons. *J. Appl. Phys.* **2012**, *111* (5), 054501.
(26) Sang, M.; Shin, J.; Kim, K.; Yu, K. J. Electronic and Thermal Properties of Graphene and Recent Advances in Graphene Based Electronics Applications. *Nanomaterials* **2019**, *9* (3), 374.
(27) Yee, S. K.; Malen, J. A.; Majumdar, A.; Segalman, R. A. Thermoelectricity in Fullerene−Metal Heterojunctions. *Nano Lett.* **2011**, *11* (10), 4089−4094.
(28) Gómez, R.; Segura, J. L.; Martín, N. Highly Efficient Light-Harvesting Organofullerenes. *Org. Lett.* **2005**, *7* (4), 717−720.
(29) Bahr, J. L.; Yang, J.; Kosynkin, D. V.; Bronikowski, M. J.; Smalley, R. E.; Tour, J. M. Functionalization of Carbon Nanotubes by Electrochemical Reduction of Aryl Diazonium Salts: A Bucky Paper Electrode. *J. Am. Chem. Soc.* **2001**, *123* (27), 6536−6542.
(30) Hernandez, Y.; Nicolosi, V.; Lotya, M.; Blighe, F. M.; Sun, Z.; De, S.; McGovern, I. T.; Holland, B.; Byrne, M.; Gun'Ko, Y. K.; Boland, J. J.; Niraj, P.; Duesberg, G.; Krishnamurthy, S.; Goodhue, R.; Hutchison, J.; Scardaci, V.; Ferrari, A. C.; Coleman, J. N. High-yield

production of graphene by liquid-phase exfoliation of graphite. *Nat. Nanotechnol.* **2008**, *3* (9), 563−568.
(31) Guan, J.; Chen, X.; Wei, T.; Liu, F.; Wang, S.; Yang, Q.; Lu, Y.; Yang, S. Directly bonded hybrid of graphene nanoplatelets and fullerene: facile solid-state mechanochemical synthesis and application as carbon-based electrocatalyst for oxygen reduction reaction. *J. Mater. Chem. A* **2015**, *3* (8), 4139−4146.
(32) Zuev, Y. M.; Chang, W.; Kim, P. Thermoelectric and Magnetothermoelectric Transport Measurements of Graphene. *Phys. Rev. Lett.* **2009**, *102* (9), 096807.
(33) Wu, Q.; Sadeghi, H.; García-Suárez, V. M.; Ferrer, J.; Lambert, C. J. Thermoelectricity in vertical graphene-C_{60}-graphene architectures. *Sci. Rep.* **2017**, *7* (1), 11680.

https://doi.org/10.1021/acs.nanolett.3c00014
Nano Lett. 2023, 23, 2726−2732